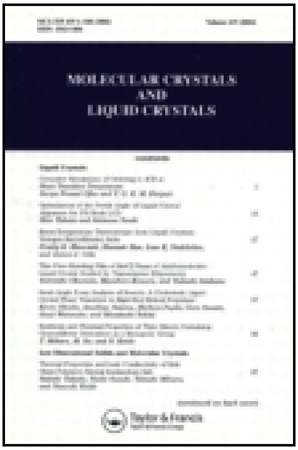

Molecular Crystals and Liquid Crystals Incorporating Nonlinear Optics
Publication details, including instructions for authors and subscription information:
http://www.tandfonline.com/loi/gmcl17

Charge Carrier Photogeneration in Poly(phenylacetylene)

J. Pfleger [a] , S. Nešpůrek [a] & J. Vohlidal [a] [b]

[a] Institute of Macromolecular Chemistry, Czechoslovak Academy of Sciences, 162 06, Prague 616, Czechoslovakia

[b] Department of Physical Chemistry, Charles University, 128 40, Prague 2, Czechoslovakia

To cite this article: J. Pfleger , S. Nešpůrek & J. Vohlidal (1989): Charge Carrier Photogeneration in Poly(phenylacetylene), Molecular Crystals and Liquid Crystals Incorporating Nonlinear Optics, 166:1, 143-156

To link to this article: http://dx.doi.org/10.1080/00268948908037146

Mol. Cryst. Liq. Cryst., 1989, Vol. 166, pp. 143–156
Reprints available directly from the publisher
Photocopying permitted by license only

Printed in the United States of America

Charge Carrier Photogeneration in Poly(phenylacetylene)

J. PFLEGER, S. NEŠPŮREK and J. VOHLÍDAL†

Institute of Macromolecular Chemistry, Czechoslovak Academy of Sciences, 162 06 Prague 616, Czechoslovakia

(*Received January 26, 1988; in final form March 19, 1988*)

Pulsed photoconduction in poly(phenylacetylene) (PPA) has been studied between 220–700 nm. The photoconduction threshold has been detected at 410 nm, although the film absorption extends up to 550 nm. The action spectrum of the photocarrier generation efficiency shows a steep rise in the range 300–400 nm and a beginning of a plateau at shorter wavelengths. It is suggested that the mechanism of photogeneration is intrinsic by nature. The thermal activation of photogeneration suggests that the experimental results can be described within the framework of the ballistic model. The dissociation of electron-hole pairs is in a good agreement with predictions based on the Onsager theory of geminate recombination. From the temperature dependence as well as from the field dependence of the quantum yield, the pair separation distance was obtained as *ca* 2.2 nm. The fraction of absorbed photons which produce thermalized electron-hole pairs is close to 2×10^{-2} charges per photon.

INTRODUCTION

Although much new physical information has emerged over the years in the area of organic compounds, relatively few have found application in active devices developed by electronics industries. Their potential use in low cost photovoltaic cells has however stimulated an interest in their electronic properties, particularly those related to photogeneration and photoconduction. The photogeneration of charge carriers in organics has been studied for a long time, but details of this process are not yet well understood. Intrinsic photogeneration has been studied in some detail for anthracene,[1-5] and one of the major achievements of these studies is the demonstration of the applicability of the Onsager model[6] for the field assisted dissociation of a pair of charges, and thus a description of the electric field dependence of the photogeneration yield. The Onsager model was also applied to explain the charge carrier photogeneration in other types of molecular crystals, *e.g.* pentacene[7] and iodoform.[8] However, alternative explanations of the primary photogeneration step were also used.[9,10] A major drawback in the application of all theoretical models to experimental results is the complex character of photoconduction processes in organics. Apart from the differences between intrinsic and

---

†Department of Physical Chemistry, Charles University, 128 40 Prague 2, Czechoslovakia.

extrinsic processes which are not always easily distinguished experimentally, complications also arise due to exciton–exciton, exciton–photon or exciton–charge carrier interactions and trapping, as well as to space charge effects.

In polymers the photoconduction mechanism was studied, for example, for poly(*N*-vinylcarbazole),[11–14] polydiacetylenes,[15,16] polyacetylene,[17,18] and for molecularly doped polymers.[19–22] The photoconduction in *trans*-poly(phenylacetylene) (PPA) and in its charge-transfer complexes was studied by Kang and co-workers.[23,24] The major photoconductivity mechanism of PPA was found to be the electron injection from the electrode into defect states lying in the band gap; in the presence of light these electrons then equilibrate with the conduction states and recombination takes place with fixed holes. These authors explained the long wavelength (extended into the near-infrared) photoconduction by a photodetrapping process. Measurements of pulsed photoconductivity were done in the spectral region between 300 and 800 nm.

We were interested to find out if the intrinsic photoconduction takes place in PPA. Therefore, (i) we prolonged the spectral range of photoconduction measurements up to 220 nm, and (ii) we used a special type of sample, with SiO spacers between the metal electrodes and the PPA in order to stop the photoinjection of charge carriers. This paper describes the results of these studies in more detail. New information concerning the intrinsic photoconductivity in PPA is presented and the mechanism underlying photoconduction in thin solid films of PPA is discussed.

EXPERIMENTAL

Material

PPA was prepared by the coordination polymerization of phenylacetylene (PA), catalyzed by the metathetic catalyst $WOCl_4 + Ph_4Sn$ in benzene/dioxan solution, using a sealed glass vacuum apparatus (initial pressure of the order 10^{-4} Pa): 43.5 μmol (18.6 mg) of Ph_4Sn (tetraphenyltin) was reacted with 21.75 μmol of $WOCl_4$ in benzene (6 ml) for 15 minutes. 1,4-Dioxan (in one portion of 4 ml), followed after about 3 minutes by one drop of PA, and finally after 1 min by PA (2.2 ml), was added into the reaction mixture. The polymerization proceeded at 293 K for 1 h. The resulting PPA was precipitated from the reaction mixture by methanol (40 ml) under vacuum, reprecipitated twice under nitrogen using the solvent system toluene-methanol, washed by methanol, and dried *in vacuo* at *ca* 320 K. The polymer was weighed and sealed under vacuum in a glass ampoule; the relative yield was 80%.

The PPA thus obtained was predominantly in the *cis*-transoidal form as demonstrated by IR spectra[25] (Perkin Elmer 580 B spectrometer, KBr discs). From the ratio of peak intensities (Figure 1) at 760 cm^{-1} and at 740 cm^{-1} (which is characteristic of the *cis*-form), the content of *cis*-form was estimated to be *ca* 80%. This result agrees with the presence of the peaks at 895 cm^{-1} and 1380 cm^{-1} which

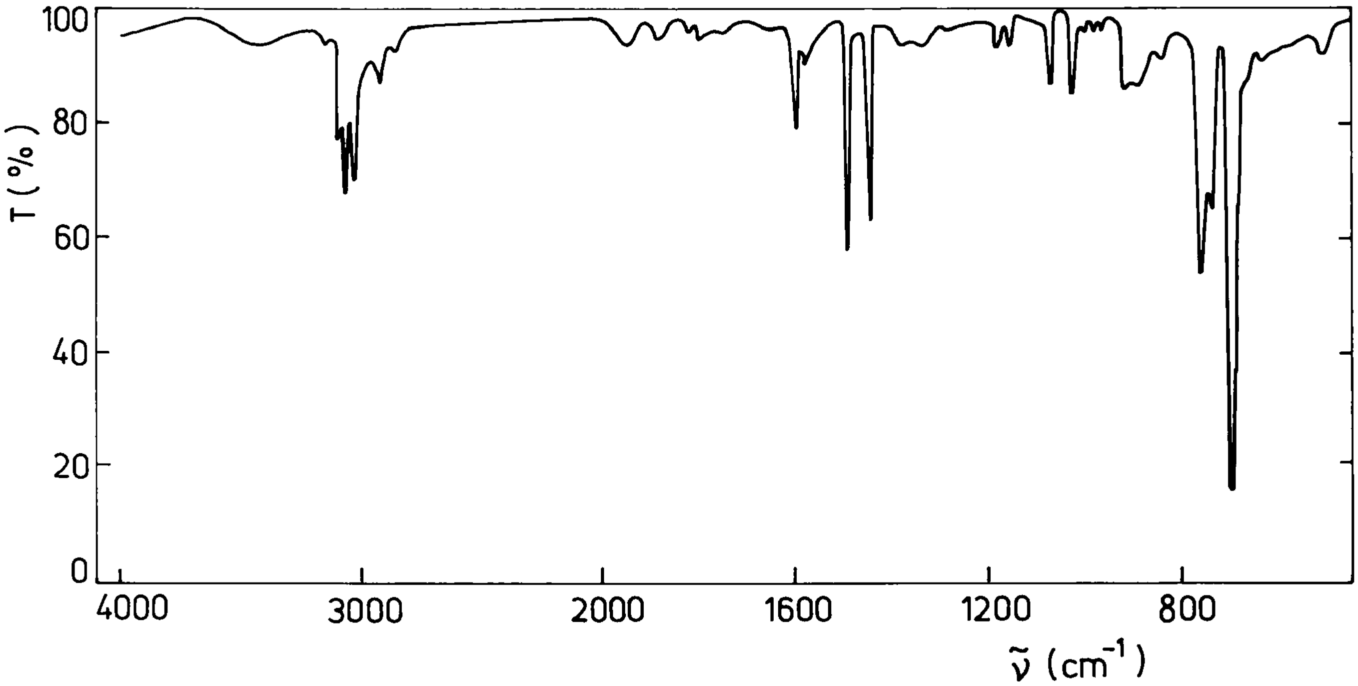

FIGURE 1 IR absorption spectrum of PPA.

are also attributed to the *cis*-form.[25] The content of *trans*-form is seen from the presence of peaks at 920 cm^{-1}, 970 cm^{-1} (the latter being assigned to the *trans* C—H out-of-plane deformation vibration[26]), and from the ratio of peaks at 1440 cm^{-1} and 1490 cm^{-1}. Using gel permeation chromatography, the average molecular weight $\overline{M}_w$ was determined as 91,000 (based on a polystyrene calibration). The polydispersity ($\overline{M}_w/\overline{M}_n$) was found to be 2.4.

Samples and measurements

Two types of sample were investigated: (*a*) a sandwich of the type G/SnO_2/PPA/Au [where G represents a glass-substrate slide (GS)] was used in electrical measurements in the dark, and (*b*) a sandwich of the type G/SnO_2/SiO/PPA/SiO/Au was employed for the measurement of pulse photoconductivity. The SiO spacers were used to stop the photoinjection of charge carriers from the metal electrode. In case (*a*) the Au electrode was 40 nm thick and prepared by vacuum deposition. For light measurements (*b*), the SiO spacers, 150 nm thick, and a semi-transparent Au electrode, 20 nm thick, were also vacuum deposited. The deposition rates were 0.1 nm s^{-1} (SiO) and 0.35 nm s^{-1} (Au). PPA films were prepared by spinning from a solution in xylene. The thickness was controlled by the spinning rate and by the solution concentration. Typical thickness values were 1 to 3 μm. The films were first dried in xylene vapour (*ca* 1 day), then in a nitrogen atmosphere (*ca* 1 day), and finally *in vacuo* (10^{-3} Pa) at 320 K for about 6 h to obtain crush-less films. The pulsed photoconductivity was measured in the bell-jar system at 10^{-4} Pa. Samples were illuminated by a Xe 457 micropulser (Xenon Corp.) through the Bausch and Lomb monochromator. The typical pulse duration was 5 μs; the number of photons in the light pulse was of the order of 10^{17} photons s^{-1} m^{-2} as measured by the EG&G 580 radiometer. To obtain the photogenerated charge ΔQ, we measured the integral of the photocurrent detected as the voltage drop ΔV by a Tektronix 564 storage oscilloscope, $\Delta Q = (\Delta U - \Delta U_b)C$, where C is the total circuit capacitance and ΔU_b is the Dember voltage. ΔU_b was usually small and the correction was negligible. The apparent quantum efficiency η' was calculated from the formula

$$\eta' = \Delta Q/e\pi, \tag{1}$$

where π is the number of photons in a single pulse incident on the PPA film and e is the unit charge. Corrections were made for the light lost in the glass slide, SnO_2 substrate electrode and the blocking SiO layer, when the substrate electrode was irradiated, or the gold top electrode and the blocking SiO layer, when the non-substrate electrode was irradiated.

The d.c. dark current was measured by a 616 Keithley electrometer. The 240 Keithley power supply was used as the power source. The electric permittivity ($\epsilon_r\epsilon_o$) was determined as 2.7×10^{-11}F m^{-1} ($\epsilon_r = 3.1$) using an RLCG transformer bridge at 1 kHz.

RESULTS

Dark characteristics

The typical current-voltage ($j \sim U$) characteristics of G/SnO$_2$/PPA/Au samples are given in Figure 2 (Au electrode being positive). The characteristics, typical of the space-charge-limited current (SCLC), were symmetric for both polarities of applied voltage. In the low-voltage range ($U < 0.1$ V, sample thickness $L = 1.1$ μm; see curve 1), the current was proportional to voltage. The transition voltage U_{x1} between the ohmic ($j \sim U$) and quadratic ranges ($j \sim U^{m+1}$, $m + 1 = 2$) was detected

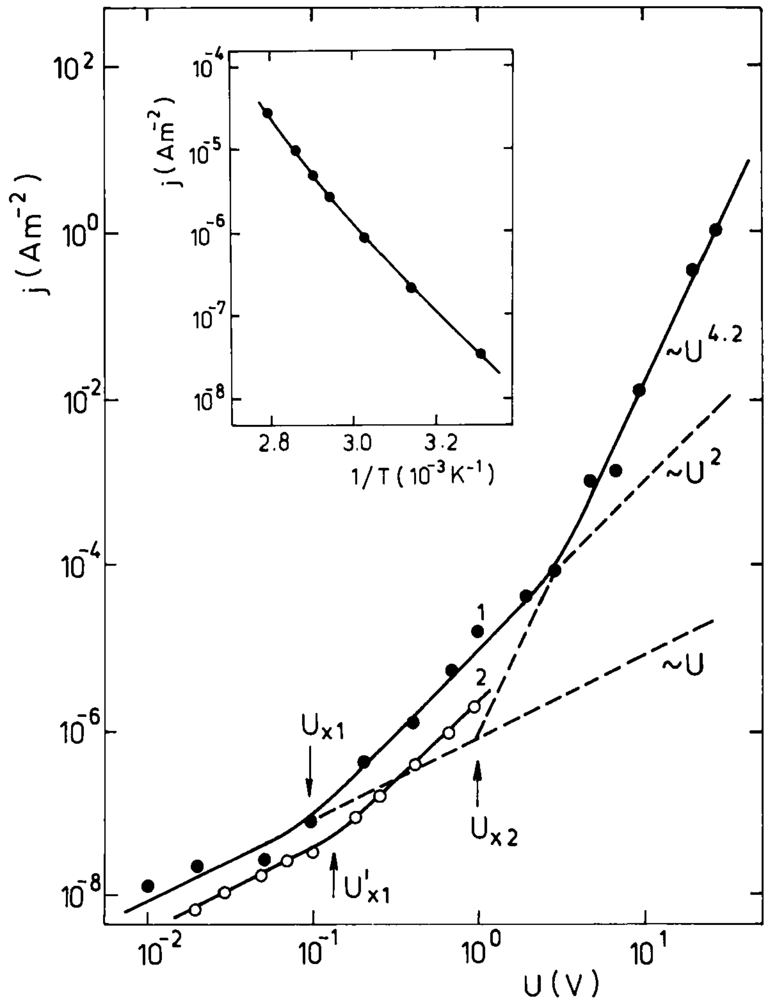

FIGURE 2 Dark current-voltage characteristics of PPA films. Temperature $T = 297$ K, sample thickness $L = 1.1$ μm (full circles), $L = 1.3$ μm (open circles). Inset: Temperature dependence of dark current; voltage applied $U = 0.1$ V.

at 0.1 V. At higher voltages ($U > 2$ V) the current followed the $j \sim U^{m+1}$ relation with the exponent $m + 1 = 4.2$.

Photoresponse

The experimental dependence of the apparent quantum efficiency η' on reciprocal temperature is given in Figure 3, and the field dependence of η' in Figure 4. The experimental dependences of η' on wavelength are given in Figure 5 for an irradiated positively biased electrode at two magnitudes of the electric field. The electron transient photocurrents were observed to be lower those for the holes, under the condition that the optical penetration depth was much less than the film thickness.

DISCUSSION

Dark characteristics

In the low-voltage region, the current was proportional to the voltage owing to the presence of thermal free carriers. The electrical conductivity was found to be 1×10^{-12} S m^{-1}. From the magnitude of the current density $j = e\bar{n}_f\mu F$, where $\bar{n}_f$ is the free carrier concentration at the thermodynamic equilibrium, μ is the mobility of the charge carriers, and F is the electric field, the product $\mu\bar{n}_f$ was determined as 6×10^6 m^{-1} V^{-1} s^{-1}. The SCL current may be observed in those cases where—after the application of voltage $U \geq U_{x1}$ to the electrodes—charge carriers are injected into the bulk of the solid and the concentration of injected carriers exceeds

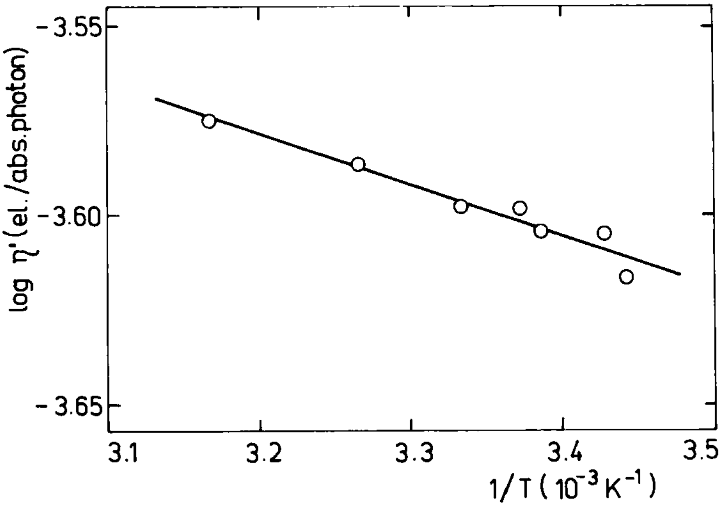

FIGURE 3 Temperature dependence of the logarithm of the apparent quantum efficiency of photogeneration η'.

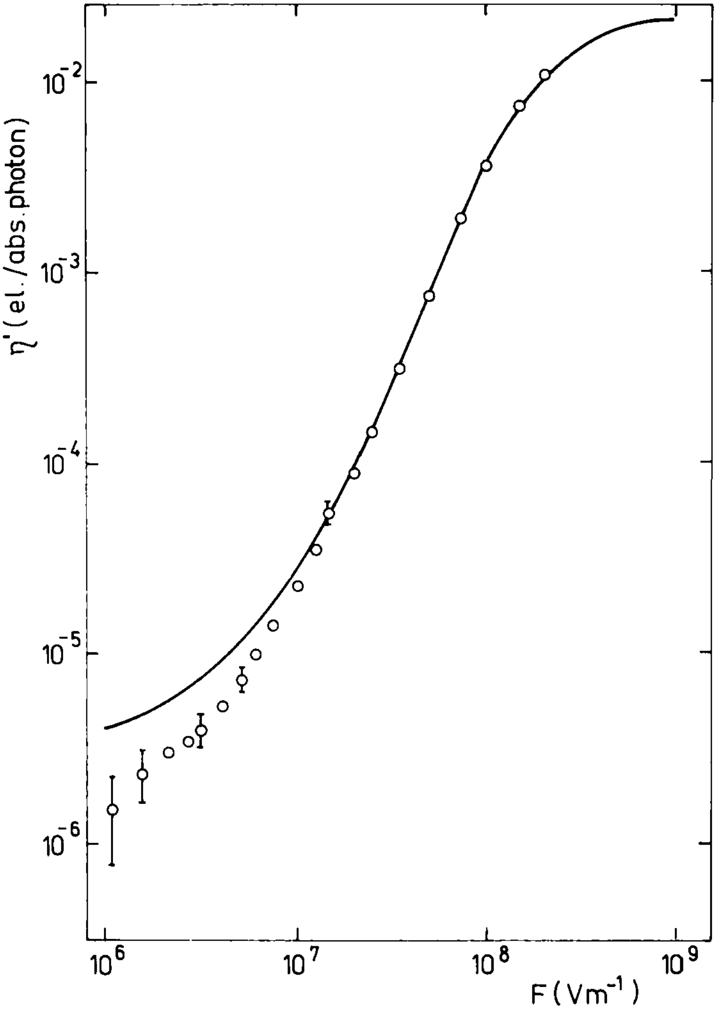

FIGURE 4 Field dependence of photogeneration efficiency in the PPA film. The excitation wavelength was 280 nm, $T = 297$ K. The solid line presents the best fit obtained using Equation (8) with the parameters $\epsilon_r = 3.1$, $\eta_o = 2 \times 10^{-2}$ charges per photon and $r_o = 2.0$ nm.

$\bar{n}_f$. The dependence of SCL current on voltage and the sample thickness L for the sandwich structure is given by the relation[27]

$$j_{\text{SCL}} = \frac{9}{8} \epsilon_r \epsilon_o \mu \theta \frac{U^2}{L^3}, \tag{2}$$

θ being the ratio of the concentration of the free, n_f, and trapped carriers, n_t,

$$\theta = \frac{n_f}{n_t + n_f} \doteq \frac{n_f}{n_t} = \frac{N_b}{N_t} \exp\left(-\frac{E_t}{kT}\right), \tag{3}$$

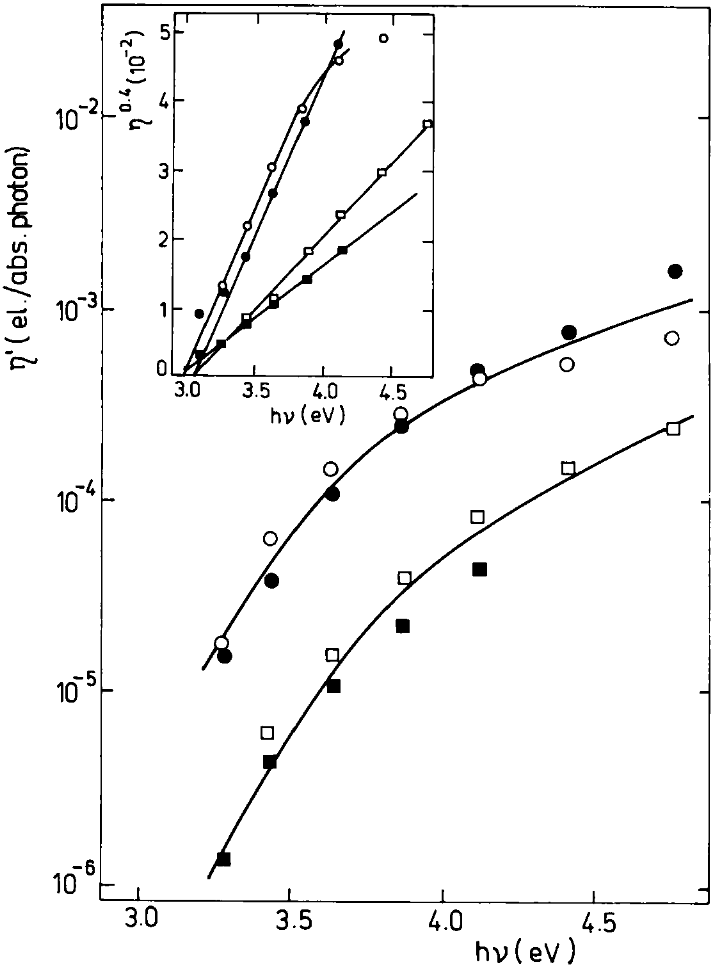

FIGURE 5 Spectral dependence of photogeneration efficiency of PPA films. Substrate SnO_2 electrode illuminated (full points), top Au electrode illuminated (open points), electric field applied $F = 1.5 \times 10^7$ V m^{-1} (squares), $F = 3 \times 10^7$ V m^{-1} (circles). The solid lines present the best fit with the parameter $R_T = 0.35$ nm. Inset: Spectral dependence of photogeneration efficiency using Equation (12).

where N_b is the effective density of states, N_t is the trap concentration, E_t is the trap depth, k is the Boltzmann constant, and T is temperature. From the quadratic part of the $j \sim U$ characteristics, the product $\mu\theta$ was determined to be 3.8×10^{-13} m^2 V^{-1} s^{-1}. From the magnitude of $U_{x1} \sim e\bar{n}_f L^2/\epsilon_r\epsilon_o\theta = 0.1$ V, the ratio $\bar{n}_f/\theta$ was obtained as 1.4×10^7 m^{-3}. The product $\mu\bar{n}_f$ was then determined to be $\mu\bar{n}_f = 6 \times 10^6$ m^{-1} V^{-1} s^{-1}.

The value of $\bar{n}_f$ was estimated from the activation energy E_a of the ohmic current density. Assuming the temperature dependence of the microscopic mobility to be weak ($\sim T^{-z}$), one can write[28,29] $E_f \approx E_a$. From experiments (see inset in Figure 2), $E_a = 0.77$ eV around room temperature. From this value the free carrier concentration can be estimated as $\bar{n}_f = 1.7 \times 10^{15}\ \mathrm{m}^{-3}$. The measurements at higher temperatures ($340\ \mathrm{K} < T < 360\ \mathrm{K}$) gave $E_a = 1.15$ eV. Using the value of $\bar{n}_f$, one can estimate the drift charge mobility of majority carriers (holes) as $\mu = 3.5 \times 10^{-8}\ \mathrm{m}^2\ \mathrm{V}^{-1}\ \mathrm{s}^{-1}$. The coefficient θ is then of the order of 10^{-5}.

The high voltage part of the $j \sim U$ dependence was characteristic of an exponential distribution of trap density in energy and the current could be described by the relation[30]

$$j_{\mathrm{SCL}} = e\mu N_b \left(\frac{\epsilon_r \epsilon_o}{eN_t'}\right)^m \left(\frac{m}{m+1}\right)^m \left(\frac{2m+1}{m+1}\right)^{m+1} \frac{U^{m+1}}{L^{2m+1}} \tag{4}$$

where N_t' is the total trap concentration, $m = T_c/T$, T_c being a temperature parameter characterizing the distribution of traps. Our experimental results gave $T_c = 975$ K. From the transition voltage U_{x2} (see Figure 2) between the ohmic $j \sim U$ and $j \sim U^{4.2}$ part of the current-voltage dependence,[30] where

$$U_{x2} \approx \frac{eL^2 N_t'}{\epsilon_r \epsilon_o} \frac{m+1}{m} \left[\frac{\bar{n}_f}{N_b}\left(\frac{m+1}{2m+1}\right)^{m+1}\right]^{1/m} \tag{5}$$

one can determine the total concentration, N_t, of exponentially distributed traps in energy,

$$N_t(E) = \frac{N_t'}{kT_c} \exp\left(-\frac{E}{kT_c}\right) \tag{6}$$

as $N_t' = 4 \times 10^{24}\ \mathrm{m}^{-3}$.

Photoresponse

The photogeneration quantum efficiency η is related to η' by the expression $\eta = \eta' b^{-1}$. The numerical carrier transition coefficient b can be determined in the case of blocking, non-injecting electrodes according to the range-limited theory.[31,32] Thus, the measured activation energy of η', $E_{\mathrm{ph}} = (0.028 \pm 0.002)$ eV, obtained at the field of $F = 3 \times 10^7\ \mathrm{V\ m}^{-1}$, consists of the activation energy of charge carrier dissociation, E_{ph}^r, the activation energy of the product $\mu\tau$ (τ being the lifetime of charge carriers), and perhaps the activation energy of photogeneration of geminate electron-hole pairs. But we have no direct information about the $\mu\tau$ product on PPA. Only a rough estimation could be made. The temperature dependence of mobility usually follows the relation $\mu = CT^{-z}$, where C and z are constants. The z value, $0 < z < 2.5$, has been generally observed[33] for many organic materials. The temperature dependence of the charge carrier life time is more problematic, because it depends on the character of the recombination centers. If N is the number per unit volume of recombination centers which can capture a free carrier, the lifetime may be expressed as $\tau = (\nu SN)^{-1}$, where ν is the thermal velocity of the carrier ($\sqrt{2kT/m}$, m being the electron mass), and S is the capture cross section of the recombination center. The magnitude of S is influenced by the potential energy variation in the vicinity of the center.

For neutral centers, the polarizability of the center is given by a quasi-long-range interaction with the carrier. A charge at a distance x from a center with polarizability α will produce a dipole moment of $\alpha e/4\pi\epsilon_r\epsilon_o x^2$. This dipole will in turn produce an attractive force of $2(\alpha e/4\pi\epsilon_r\epsilon_o x^2)\,(e/4\pi\epsilon_r\epsilon_o x^3)$ on the charge so that there is an attractive potential $V(x) = -A/x^4$, where A is a constant equal to $\alpha e^2/32(\pi\epsilon_r\epsilon_o)^2$. Different centers (impurities) in a host material have different α values. Because the radius at which the potential energy is kT varies with $T^{-1/4}$, τ will be nearly temperature independent and $\mu\tau \sim T^{-3/2}$. For attractive Coulombic centers, the capture cross-section is roughly proportional to T^{-2} as given by Rose,[34] and therefore τ is proportional to $T^{3/2}$. The $\mu\tau$ is then nearly temperature independent and cannot influence the activation energy of photogeneration. Assuming the centers in PPA to be neutral, a situation usually encountered in organic molecular solids, the corrected activation energy value of the charge carrier dissociation would be obtained as $E^r_{\mathrm{ph}} = 0.07$ eV. Here, the activation energy of photogeneration of geminate electron-hole pairs was neglected.

Batt *et al.*[35] were the first to demonstrate that for the intrinsic photogeneration of free carriers, an experimentally detectable activation energy is needed. These results show that photogeneration in anthracene crystals[1] occurs, *e.g.*, via an intermediate stage of a bonded charge pair state and its subsequent thermal dissociation, which is a thermally activated and field-assisted diffusive process.[6] The existence of the thermally activated charge carrier photogeneration was the reason why we tried to fit the experimental data in terms of the ballistic model, including the Onsager theory. According to this model, the intrinsic photogeneration in organic solids is usually depicted as a multistage process which involves: (i) photogeneration to a neutral molecular electronic state, (ii) autoionization of the excited state, resulting in the creation of a localized hole and a hot quasi-free electron, (iii) thermalization of the electron due to fast inelastic scattering, leading to the formation of a Coulomb field-bound geminate electron-hole pair [so-called charge-transfer (CT) state], and (iv) thermal dissociation of the electron-hole pair into free carriers by the Brownian motion subject to a combined Coulomb and applied field. The fraction of absorbed photons that result in bound thermalized pairs gives the primary quantum yield η_o and is often assumed to be independent of the applied field. Under this assumption, the overall field dependence of photogeneration is governed by the efficiency of the dissociation step (iv) which may be described using the solution of the Smoluchowski equation given by Onsager.[6] The photogeneration efficiency may be calculated as

$$\eta(\mathbf{F},T) = \eta_o \int f(\mathbf{r},\mathbf{R},T)\, g(r)\, d\tau, \tag{7}$$

where $f(\mathbf{r},\mathbf{F},T)$ is the dissociation probability of bound pairs separated by a distance $r = |\mathbf{r}_e - \mathbf{r}_h| = |\mathbf{r}|$, $\mathbf{r}_e$, $\mathbf{r}_h$ being radius vectors of the electron and hole, respectively, $g(\mathbf{r})$ represents the initial spatial distribution of bound pairs, and $d\tau$ is the volume element. Assuming that the distribution is spherically symmetrical and that all pairs are separated by the same distance r_o, we have $g = (4\pi r_o^2)^{-1}\,\delta\,(r - r_o)$ and integration in Equation (7) gives the overall photogeneration efficiency. Its dependence on the applied electrical field and on temperature T can be described by a modified Onsager formula,[6] which can be rewritten employing the Bessel functions[36] in the form

$$\eta(r_o,F) = \eta_o\left[1 - \frac{kT}{eFr_o}\sum_{j=0}^{\infty} I_j\left(\frac{e^2}{4\pi\epsilon_r\epsilon_o kTr_o}\right) I_j\left(\frac{eFr_o}{kT}\right)\right], \tag{8}$$

where $I_j(x)$ is a modified Bessel function of the first kind. The Coulomb energy $E_b(r_o)$ of two charges separated by the distance r_o can be approximated with a remarkably good accuracy by the Coulombic binding energy in the isotropic continuum approximation, *i.e.*,

$$E_b(r_o) = e^2/4\pi\epsilon_r\epsilon_o r_o. \tag{9}$$

The equation is valid in the zero-field approximation. After correction of the experimental value of the activation energy E'_{ph} to zero field using formula (8), $r_o = 2.3$ nm was obtained for the neutral type of recombination center. It is interesting to compare this value with the fitted r_o obtained form the experimental data for field dependence of η', given in Figure 4. The best fit parameters obtained were $r_o = 2.0$ nm and $\eta_o = 2 \times 10^{-2}$ charges per photon. These results set the value of the zero-field quantum efficiency of photogeneration at about 10^{-6} charges per photon. The low-field region ($f < 10^7$ V m^{-1}) of the η' *vs.* F dependence is rather dubious, owing to a large experimental inaccuracy. A small amount of trapped charge results in a field in the generation region that is vastly different from the applied field. The film had to be "rested" for several days between measurements to get out of the charge present, especially when the blocking spacers were used. A large error can be expected at low applied fields, under the usual conditions where a 10 min period of resting was used between measurements.

On the basis of the η' *vs.* F dependence we believe Onsager's theory to provide a completely satisfactory explanation of the experimental results on photogeneration in this material. As expected, the efficiency of dissociation depends on the initial distance between the oppositely charged carriers. The distance, according to the first step of the ballistic model—thermalization, depends on the excess of excitation energy, and is thus the reason for the wavelength dependence of η'. The process of separation involves a loss by phonon emission of the excess kinetic energy of the carrier pair. In a material where the mean free path is comparable to the intermolecular spacing, the motion during this process is expected to be diffusive and the separation distance r_o at the end of the thermalization time t_t will be given[37] by the relation $r_o = \{Dt_t\}^{1/2}$, where D is the diffusion coefficient. From the relation of k-conservation in inelastic scattering, the rate of loss of energy in an amorphous material is expected to reach its maximum at a phonon frequency multiplied by a typical phonon energy. The excess of kinetic energy E_k to be dissipated is then taken to be an excess over the local Coulomb potential as[37]

$$E_k = h\nu - E_g + \frac{e^2}{4\pi\epsilon_r\epsilon_o r}, \tag{10}$$

where E_g is the energy gap. The time necessary to dissipate this energy is then $t_t = E_k/h\nu_p^2$, where ν_p is the phonon frequency. The electron-hole separation distance r_o at the end of the thermalization process is then given as $r_o = R_T(E_k/kT)^{1/2}$, with $R_T = (kTD/h\nu_p^2)^{1/2}$. Using Equation (10), r_o is then given by the relation

$$r_o = R_T\left(\frac{h\nu - E_g + e^2/4\pi\epsilon_r\epsilon_o r_o}{kT}\right)^{1/2} \tag{11}$$

The experimental plot of η' *vs.* $h\nu$ given in Figure 5 was fitted using expressions (8) and (11), yielding $R_T = 0.35$ nm. The fitted spectral responses are given in Figure 5 as full lines. The value of the band gap energy was taken as the threshold value $E_g = (3.0 \pm 0.1)$ eV from the dependence[38]

$$\eta(h\nu) = A(h\nu - E_g)^n, \tag{12}$$

where $n \approx 2.5$. The test of this dependence is presented in the inset in Figure 5. This value differs from the determined value of the "band gap" from the optical spectrum, where the value of $E_g^o = 2.2$ eV was determined.

The absence of intrinsic photogeneration in PPA at wavelengths longer than *ca* 400 nm, *i.e.*, in the range where PPA still has a strong absorption (see Figure 6), indicates that only the higher-lying states may be involved in autoionization, if it takes place at all. The presence of a plateau in the spectral dependence of photoconduction (and thus in the wavelength dependence of r_o) is explained assuming—similar to the model of Noolandi and Hong[10]—that absorption to higher energetic states is followed by a rapid dissipation of excess of energy due to radiationless transitions. The second excited state thus generated autoionizes to a CT state with a radius of approximately 2.0 nm. Further dissociation occurs according to the Onsager model. A similar trend of increasing photoresponse for wavelengths shorter than 400 nm can be seen also from the observations of Kang *et al.*[23,24] The photoresponse at longer wavelengths with a weakly pronounced maximum at *ca* 650 nm was discussed by Kang *et al.* as the photodetrapping of shallow traps below the conduction band.

CONCLUSION

Results presented in this study show that the high field limit of intrinsic photogeneration efficiency in PPA is 2×10^{-2} charges per photon. The zero field photogeneration efficiency extrapolated from the present results, being *ca* 10^{-6} charges per photon, results from a relatively short thermalization distance r_o = 2.0 nm. The Onsager model seems to be adequate for explaining the experimental dependences of quantum efficiency on the electric field and on temperature at shorter wavelengths; however, details of the formation of initial charge carrier pairs are still open to discussion.

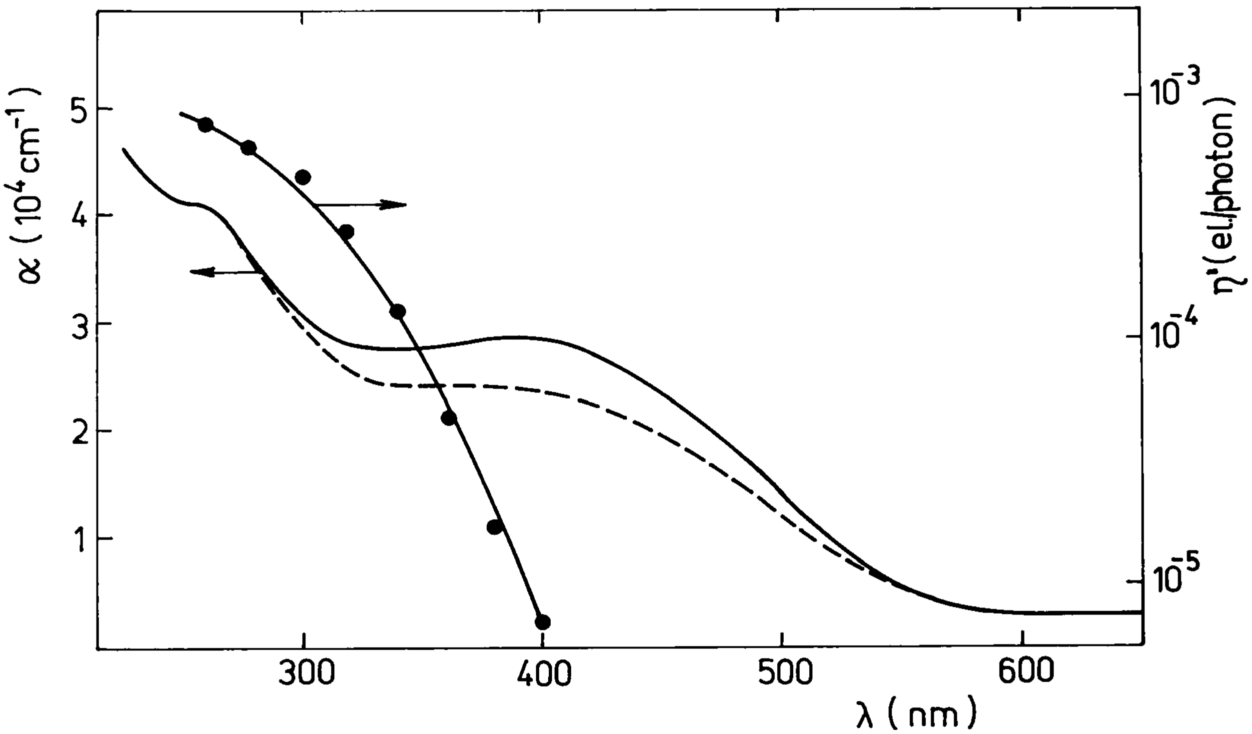

FIGURE 6 Spectral dependence of the absorption coefficient α (full line and dashed line) and of apparent quantum efficiency η' (full line with circles) of the PPA film. Full line: fresh sample; dashed line: sample after 5 min. exposure to UV light in the air.

References

1. G. Castro and J. F. Horning, *J. Chem. Phys.*, **42**, 1459 (1965).
2. R. R. Chance and C. L. Braun, *J. Chem. Phys.*, **59**, 2269 (1973).
3. R. R. Chance and C. L. Braun, *J. Chem. Phys.*, **64**, 3573 (1976).
4. K. Kato and C. L. Braun, *J. Chem. Phys.*, **72**, 172 (1980).
5. L. E. Lyons and K. A. Milne, *J. Chem. Phys.*, **65**, 1474 (1976).
6. L. Onsager, *Phys. Rev.*, **54**, 554 (1938).
7. E. A. Silinsh and A. J. Jurgis, *Chem. Phys.*, **94**, 77 (1985).
8. S. Nešpůrek, A. Samoč, M. Samoč and J. Sworakowski, *J. Chem. Phys.*, **79**, 3104 (1983).
9. P. J. Bounds and W. Siebrand, *Chem. Phys. Lett.*, **75**, 414 (1980).
10. J. Noolandi and K. M. Hong, *J. Chem. Phys.*, **70**, 3230 (1979).
11. P. M. Borsenberger and A. I. Ateya, *J. Appl. Phys.*, **49**, 4035 (1978).
12. G. Pfister and D. J. Williams, *J. Chem. Phys.*, **61**, 2416 (1974).
13. S. Nešpůrek, V. Cimrová, and B. Klein-Szymanska, "*Morphology of Polmyers*," (Ed. B. Sedláček), Walter de Gruyter, Berlin, New York, 1986, p. 681.
14. K. Okamoto and A. Haya, *Bull. Chem. Soc. Jpn.*, **57**, 1626 (1984).
15. V. Seiferheld, B. Ries and H. Bässler, *J. Phys. C: Solid State Phys.*, **16**, 5189 (1983).
16. K. J. Conovan and E. G. Wilson, *J. Phys. C: Solid State Phys.*, **19**, L357 (1986).
17. J. Orenstein, Z. Varedeny, G. L. Baker, G. Eagle and S. Etemad, *Phys. Rev. B***30**, 786 (1984).
18. H. Kiess, R. Keller, D. Baeriswyl and G. Harbeke, *Solid State Commun.*, **44**, 1443 (1982).
19. P. M. Borsenberger, L. E. Contois and D. C. Hoestery, *Chem. Phys. Lett.*, **56**, 574 (1978).
20. P. M. Borsenberger, L. E. Contois and A. I. Ateya, *J. Appl. Phys.*, **50**, 914 (1979).
21. T. E. Goliber and J. H. Perlstein, *J. Chem. Phys.*, **80**, 4162 (1984).
22. J. Mort and G. Pfister, *Polym.-Plast. Technol. Eng.*, **12**, 89 (1979).
23. E. T. Kang, P. Ehrlich and W. A. Anderson, *Mol. Cryst. Liq. Cryst.*, **106**, 305 (1984).
24. E. T. Kang, P. Ehrlich, A. P. Bhatt and W. A. Anderson, *Macromolecules*, **17**, 1020 (1984).
25. C. I. Simionescu, V. Percec and S. Dimitrescu, *J. Polym. Sci.*, *Polym. Chem. Ed.*, **15**, 2497 (1977).
26. A. Furlandi, I. Collamati and G. Sartori, *J. Organometal. Chem.*, **17**, 463 (1969).
27. M. A. Lampert, *Phys. Rev.*, **103**, 1648 (1956).
28. F. Schauer, O. Zmeškal and S. Nešpůrek, *Phys. Status Solidi* (*a*), **85**, 619 (1984).
29. O. Zmeškal, F. Schauer and S. Nešpůrek, *J. Phys. C: Solid State Phys.*, **18**, 1873 (1985).
30. P. Mark and W. Helfrich, *J. Appl. Phys.*, **33**, 205 (1962).
31. Z. D. Popovic and J. H. Sharp, *J. Chem. Phys.*, **66**, 5076 (1977).
32. S. Nešpůrek, R. H. G. Hart, J. S. Bonham and L. E. Lyons, *Austr. J. Chem.*, **38**, 1061 (1985).
33. K. C. Kao and W. Hwang, "*Electrical Transport in Solids*," Pergamon Press, Oxford, 1981, p. 14.
34. A. Rose, "*Concepts in Photoconductivity and Allied Problems*," Wiley, New York, London, 1963, p. 123.
35. R. H. Batt, C. L. Braun and J. F. Horning, *J. Chem. Phys.*, **49**, 1967 (1968).
36. A. Mozumder, *J. Chem. Phys.*, **60**, 4300 (1974).
37. J. C. Knights and E. A. Davis, *J. Phys. Chem. Solids*, **35**, 543 (1974).
38. E. A. Silinsh, "*Organic Molecular Crystals*," Springer-Verlag, Berlin, Heidelberg, New York, 1980, p. 114.